

A cloned horse born to its dam twin

A birth announcement calls for a rethink on the immunological demands of pregnancy.

Several animal species, including sheep, mice, cattle, goats, rabbits, cats, pigs and, more recently, mules¹ have been reproduced by somatic cell cloning, with the offspring being a genetic copy of the animal donor of the nuclear material used for transfer into an enucleated oocyte. Here we use this technology to clone an adult horse and show that it is possible to establish a viable, full-term pregnancy in which the surrogate mother is also the nuclear donor. The cloned offspring is therefore genetically identical to the mare who carried it, challenging the idea that maternal immunological recognition of fetal antigens influences the well-being of the fetus and the outcome of the pregnancy.

We derived equine fibroblast cell lines from skin biopsies taken from one Arabian thoroughbred male and one Haflinger female. Oocytes were obtained by *in vitro* maturation of follicular oocytes recovered from equine ovaries retrieved from abattoirs. After removal of the nucleus and zona material, embryos were reconstructed by cell fusion with the fibroblasts. Only fused embryos (97%) were activated and cultured *in vitro* to the blastocyst stage; these were then transferred into recipient mares (see supplementary information).

We cultured 513 and 328 successfully fused reconstructed embryos from the male and the female cell lines, respectively. In total, 22 blastocysts developed, 8 from the male and 14 from the female cell line. Of these, eight blastocysts from the male cell line and nine from the female line were transferred non-surgically into nine recipients. Two of the cloned embryos that were reconstructed with female cells were transferred into the Haflinger mare from which the cell line was derived.

Overall, four single pregnancies were diagnosed by ultrasonography after 21 days of gestation. Two were lost soon afterwards and one aborted at 187 days of gestation; the fourth, however, was carried to term (336 days) and a healthy female foal was born naturally on 28 May 2003 (birth weight, 36 kg). Remarkably, this cloned foal was born from the same Haflinger mare who was the original cell-line donor (Fig. 1).

To confirm the genetic identity of the foal and her mother, we analysed DNA from blood leukocytes from both animals and from the placenta. Comparison of 12 equine-specific microsatellite loci (Stock-Marks kit, Perkin-Elmer, Applied Biosystems) confirmed that DNA from the foal and from the placenta was identical to that of the recipient mare.

Our cloning procedure was relatively efficient, as one live foal was produced from four pregnancies, although there was high developmental failure from the cleavage stage to blastocyst (8 of 467 and 14 of 286 developed in the male and female cell lines, respectively) and early implantation. This success was aided by advances in assisted reproduction in the horse², particularly at the oocyte-activation stage, when protein synthesis and phosphorylation must both be inhibited³, and in the refinement of the zona-free manipulation technique^{4,5}.

The remarkable birth of a live foal from its genetically identical recipient is at odds with the idea that the maintenance of gestation depends on immunological recognition of the pregnancy by the mother, based on evidence that abortion can result from inadequate recognition of fetal antigens⁶.

Furthermore, our result adds the horse to the list of mammals that have so far been successfully cloned from an adult somatic cell. In principle, cloning could enable gelding champions to contribute their genotype to future generations, as well as opening up an opportunity to verify the reproducibility of traits such as character and sporting performance.

Cesare Galli, Irina Lagutina, Gabriella Crotti, Silvia Colleoni, Paola Turini, Nunzia Ponderazzo, Roberto Duchi, Giovanna Lazzari

Laboratorio di Tecnologie della Riproduzione, CIZ srl, Istituto Sperimentale Italiano Lazzaro Spallanzani, 26100 Cremona, Italy



Figure 1 The cloned foal, named Prometea, with its genetically identical mother seven days after birth. The cells used for cloning were derived from a skin biopsy of the mare. The enucleated oocytes were obtained by *in vitro* maturation and removal of the nucleus from oocytes recovered from horse ovaries from an abattoir. After embryo reconstruction by micromanipulation and cell fusion, the cleaved embryos were cultured *in vitro* to the blastocyst stage. Two of the derived embryos were transferred into the mare donor of the cell line. A single pregnancy was established and was carried to term with the birth of a female foal who is genetically identical to her surrogate mother.

e-mail: cesare@galli2.191.it

1. Woods, G. L. *et al. Science* doi:10.1126/science.1086743 (2003).
2. Galli, C. *et al. Theriogenology* **58**, 705–708 (2002).
3. Lazzari, G., Mari, G. & Galli, C. *J. Reprod. Fert. Ser.* **28**, 73 (2002).
4. Lagutina, I. *et al. Theriogenology* **59**, 269 (2003).
5. Wilmut, I. *Cloning and Stem Cells* **5**, 1–2 (2003).
6. Szekeres-Bartho, J. *Int. Rev. Immunol.* **21**, 471–495 (2002).

Supplementary information accompanies this communication on Nature's website.

Competing financial interests: declared none.

Lithium-ion batteries

Runaway risk of forming toxic compounds

Lithium-ion batteries are stabilized by an ultrathin protective film that is 10–50 nanometres thick and coats both electrodes. Here we artificially simulate the 'thermal-runaway' conditions that would arise should this coating be destroyed, which could happen in a battery large enough to overheat beyond 80 °C. We find that under these conditions the reaction of the battery electrolyte with the material of the unprotected positive electrode results in the formation of toxic fluoro-organic compounds. Although not a concern for the small units used in today's portable devices, this unexpected chemical hazard should be taken into account as larger and larger lithium-ion batteries are developed,

for example for incorporation into electric-powered vehicles.

Lithium-ion cells are now ubiquitous in consumer electronics. The negative electrode consists of lithium in graphite and the positive electrode contains lithium and a transition metal such as cobalt, nickel or manganese. However, with a lead voltage of about 4 volts, no electrolyte is thermodynamically stable towards either electrode, so the operation of these batteries relies on a combination of the ethylene carbonate and LiPF₆ (LiBF₄)-based electrolyte producing a continuous film that ensures sufficient ionic conductivity and provides electronic insulation to protect the electrodes.

Above 80 °C, thermal runaway can occur spontaneously as a result of the break-up of this protective film. Today's commercial batteries are checked by electronic monitoring of individual cells and by a self-clogging polyolefin separator to prevent overheating,

Table 1 Product yields from different lithium compounds

| Run | A | Solvent | B | Organo-F yield (%) |
|-----|---|----------|----------------------------------|--------------------|
| 1 | LiPF ₆ | EC | — | 0 |
| 2 | LiPF ₆ | EC | LiCoO ₂ | 80 |
| 3 | Li[(CF ₃ SO ₂) ₂ N] | EC | LiCoO ₂ | 0 |
| 4 | LiBF ₄ | EC | LiCoO ₂ | 80 |
| 5 | LiBF ₄ | EC | LiMn ₂ O ₄ | 80 |
| 6 | LiBF ₄ | EC | LiNiO ₂ | 80 |
| 7 | LiPF ₆ | EC + DMC | LiCoO ₂ | 35 |

Yields of fluoro-organics are shown for ethylene carbonate reacting with lithium compounds A and B at 240 °C for 30–60 min in different solvents. EC, ethylene carbonate; DMC, dimethyl carbonate.

and their failure rate has dropped to about 0.3 per million. The consequences of runaway reactions have so far focused mainly on the risks of fire, burns and the release of hydrogen fluoride.

The compound 2-fluoroethanol is highly toxic (the 50%-lethal dose, LD₅₀, in mice is 0.1 mg kg⁻¹) and is readily formed by nucleophilic attack of fluoride ion on ethylene carbonate¹. Although no example of electrophilic fluorination using coordination anions such as LiPF₆ is known, we investigated whether a similar reaction could occur by this route.

Ethylene carbonate and LiPF₆ alone do not form fluoro-organics, but these are generated in abundance when any of the positive-electrode materials (Li_xMO₂, where M is Co, Ni or Mn) is also present. Gas chromatography with mass spectrometry (110 mass units) indicates that the fluoroethanol ether is formed under these conditions: two moles of ethylene carbonate react with one mole of LiPF₆ to yield one mole each of (FCH₂CH₂)₂O, LiF and volatile POF₃ (boiling point, -39.7 °C), providing the driving force with the loss of two moles of CO₂.

Ethylene oxide (formed by the loss of CO₂ from ethylene carbonate and catalysed by the transition metal) is a likely transient intermediate. The compound bis-(2-fluoroethyl)-ether, which has an LD₁₀₀ in rats of 10 mg kg⁻¹ (estimated LD₅₀ of 4 mg kg⁻¹; ref. 2), represents 80% of the total fluoro-chemicals in runs 2 and 4–6, which are summarized in Table 1. The carbon anion with covalently bonded fluorine (CF₃⁻) is inert.

Our experiments are *ex situ* and relate only to the reaction of electrolyte with the material of the positive electrode. However, the conditions triggering the ring-opening fluorination of ethylene carbonate could easily occur in large batteries (weighing more than 500 g), such as those proposed for use in electric vehicles, where a short-circuit might cause the temperature in the electrolyte to rise instantly above 250 °C. Although these batteries are in principle highly desirable for saving energy and preventing pollution and for CO₂ abatement, their safety should be rigorously investigated under protected conditions. Further exploration of the chemicals evolved in runaway reactions should be undertaken with

extreme caution and only where *ad hoc* facilities are available.

Amer Hammami, Nathalie Raymond, Michel Armand

Laboratoire International sur Les Matériaux Electro-actifs CNRS-UdM, UMR 2289, Université de Montréal, PO Box 6122, Montréal, Québec H3C3J7, Canada
e-mail: michel.armand@umontreal.ca

1. Bergmann, E. D. & Shahak, I. *J. Chem. Soc. C*, 899–900 (1966).
2. Gitter, S., Blank, I. & Bergmann, E. D. *K. Ned. Akad. Wetenschap. Proc. C* 56, 427–430 (1953).

Competing financial interests: declared none.

Palaeontology

Spider-web silk from the Early Cretaceous

The use of viscid silk in aerial webs as a means to capture prey was a key innovation of araneoid spiders and has contributed largely to their ecological success¹. Here I describe a single silk thread from a spider's web that bears glue droplets and has been preserved in Lebanese amber from the Early Cretaceous period for about 130 million years. This specimen not only demonstrates the antiquity of viscid silk and of the spider superfamily Araneoidea, but is also some 90 million years older than the oldest viscid spider thread previously reported in Baltic amber from the Eocene epoch².

The silk glands that produce the gluey coating on viscid silk may be the best single character to define the Araneoidea, the superfamily that includes all cribellate orb-weavers and the comb-footed spiders

(Theridiidae)³. A fossil spider from the Early–Middle Jurassic (which is about 190 Myr old) has been described — on the basis of characters other than its silk-producing glands — as belonging to the Araneoidea⁴, and araneoid spiders have been recorded from the Early Cretaceous^{5,6}.

Spiders are known to have been able to produce silk since the Mid-Devonian period, about 410 Myr ago⁷. It is unclear, however, how today's intricate araneoid webs with viscid silk evolved from the probably primitive silk that was used by Devonian spiders. Current ideas about the evolution of aerial webs and of viscid silk are based on the phylogeny of the spiders, which in turn is based on morphological characters — mostly genitalic ones — whose evolution is generally not directly linked to the spider's ability to build webs or to produce viscid silk.

The present specimen (C19/2, held at the Staatliches Museum für Naturkunde in Stuttgart, Germany) was collected by Dieter Schlee in 1969 from amber beds located near Jezzine in Lebanon. These deposits are dated to the Hauterivian (about 127–132 Myr) and represent the oldest known amber with insect inclusions⁸.

The specimen contains a single thread of about 4 mm in length, which shows a striking resemblance to recent araneoid spider threads, with 38 distinct fossilized glue droplets arranged at regular intervals along two sections (Fig. 1a). The thread diameter (3 µm) and the size (7–29 µm), density (22 droplets per mm), arrangement (small droplets alternating with larger ones) and shape (semi-transparent globules, slightly elongated along the thread) of most glue droplets (Fig. 1b) closely match those in recent araneoid webs⁹. Some droplets have a larger diameter of up to 85 µm (Fig. 1c), probably as a result of water uptake from the resin (araneoid glue droplets are highly hygroscopic¹⁰) and subsequent merging with neighbouring droplets.

As the specimen contains only a single thread, we cannot identify with certainty the type of web of which this thread was a part. It may have been part of an orb-web or of a gum-footed web, as built by some

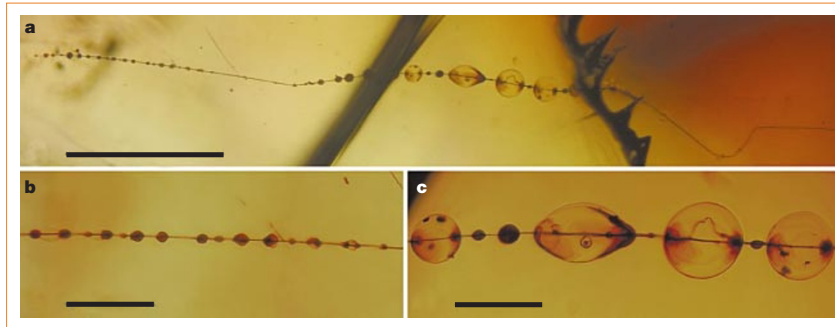


Figure 1 Fossil araneoid spider thread with glue droplets in Lebanese amber. **a**, Overall view: the thread runs at an angle of 50° to the upper surface of the amber; the left-hand end of the thread reaches the lower surface of the amber. **b**, A region of the thread showing regularly arranged glue droplets. **c**, Distended glue droplets with clearly visible core threads. Scale bars: **a**, 500 µm; **b**, **c**, 100 µm.

Kinetics

Gaussian statistics in granular gases

A kinetic theory^{1,2} of granular media, analogous to that described by Maxwell–Boltzmann statistics for molecular gases and liquids^{3,4}, has long been sought in the quest for a continuum theory. Here we present results from a two-layer, vertically vibrated granular system, in which an oscillating plate drives a horizontal layer of heavy grains, which in turn drives an overlying horizontal layer of lighter grains. In the second layer, but not in the first, we find that the velocity distributions are gaussian — a result that is observed for a wide variety of driving and density parameters, indicating that the second layer’s behaviour is much more gas-like than was previously seen in driven granular media. This similarity to molecular gases brings a kinetic theory of granular media a step closer.

Attempts to apply a kinetic theory to granular media have been undermined by their observed non-gaussian velocity distributions^{5–12}, which are inconsistent with Maxwell–Boltzmann statistics. We have designed a set-up (Fig. 1a) in which a two-layer granular medium is shaken vertically on a horizontal plate. The plate moves as

$x(t) = A \times \sin(2\pi ft)$, which corresponds to a dimensionless acceleration of $\Gamma = (2\pi f)^2/g$ where f is the oscillation frequency, A is the oscillation amplitude and g is the acceleration due to gravity. The plate’s circular sidewall is topped by a Plexiglas plate coated with a conducting film to prevent electrostatic build-up.

The granular medium is composed of two types of grain. The first layer above the oscillating plate is made up of dimeric ‘grains’, each consisting of two 3.2-mm steel spheres connected by a metal rod made from a cut bank chain (as used by banks to prevent patrons from removing their pens); each dimer has a mass (m_d) of 185 ± 7 mg. The second layer is composed of monomeric grains that are plastic (Delrin) spheres of diameter 3.175 mm and mass (m_m) 22.9 ± 0.2 mg. The difference in mass between the grains of the first and second layers keeps the dimers and monomers separated, as the monomers cannot displace the heavier dimers.

The system is prepared by building a single layer of dimers on the plate (Fig. 1b) and placing a second layer of Delrin spheres on top (Fig. 1c). We define the coverage, c , of the layer to be the proportion of the maximum number of grains that could theoretically be packed into the area if wall effects are ignored. We collected data at $c = 0.4, 0.6$ and

$0.8, f = 50, 70$ and 90 Hz, and at dimensionless accelerations (Γ) of 1.75, 2.00 and 2.25.

Velocities in the first and second layers can be measured simultaneously by high-speed digital photography, although measurement by this method in the first layer becomes difficult at high coverage. The two layers show very different velocity distributions (Fig. 1d): in the first, the distribution tails are non-gaussian (typical deviation from gaussian flatness is about 1.5, which is consistent with earlier results^{5–12}), whereas in the second layer the distribution is much more gaussian (typical deviation from gaussian flatness is less than 0.1).

The gaussian-velocity distributions in the second layer indicate that the grains are more ‘gas-like’ in their behaviour than has previously been found in vibrated granular media. This is probably due to the way in which energy is transferred to the second layer through collisions with the first layer throughout the shaking cycle. By contrast with earlier experiments, the gaussian velocity distribution of the second layer is observed at all coverages, frequencies and accelerations. Our system may therefore be ideally suited to developing a kinetic theory of granular gases.

G. W. Baxter*, J. S. Olafsen†

*School of Science, Penn State Erie, The Behrend College, Erie, Pennsylvania 16563, USA

†Department of Physics and Astronomy, University of Kansas, Lawrence, Kansas 66045, USA

e-mail: jolafsen@ku.edu

- Haff, P. K. *J. Fluid Mech.* **134**, 401–430 (1983).
- Grossman, E. L., Zhou, T. & Ben-Naim, E. *Phys. Rev. E* **55**, 4200–4206 (1997).
- Huang, K. *Statistical Mechanics* (Addison-Wesley, Boston, 1963).
- Batchelor, G. K. (ed.) *An Introduction to Fluid Dynamics* (Cambridge Univ. Press, Cambridge, 1983).
- Olafsen, J. S. & Urbach, J. S. *Phys. Rev. Lett.* **81**, 4369–4372 (1998).
- Olafsen, J. S. & Urbach, J. S. *Phys. Rev. E* **60**, R2468–R2471 (1999).
- Losert, W., Cooper, D. G. W., Delour, J., Kudrolli, A. & Gollub, J. P. *Chaos* **9**, 682–690 (1999).
- Kudrolli, A., Wolpert, M. & Gollub, J. P. *Phys. Rev. Lett.* **78**, 1383–1386 (1997).
- Kudrolli, A. & Henry, I. *Phys. Rev. E* **62**, R1489–R1492 (2000).
- Blair, D. L. & Kudrolli, A. *Phys. Rev. E* **64**, R050301 1–4 (2001).
- Rouyer, F. & Menon, N. *Phys. Rev. Lett.* **85**, 3676–3679 (2000).
- Atwell, J. & Olafsen, J. S. *Phys. Rev. E* (submitted).

Competing financial interests: declared none.

corrigendum

A cloned horse born to its dam twin

Cesare Galli, Irina Lagutina, Gabriella Crotti, Silvia Colleoni, Paola Turini, Nunzia Ponderato, Roberto Duchi, Giovanna Lazzari
Nature **424**, 635 (2003)

It has been drawn to our attention that a successful pregnancy in a goat carrying a genetically identical conceptus has previously been reported¹; complete immune compatibility was demonstrated between the mother and her kid twin (both generated by splitting a single embryo). These findings also indicate that a maternal immune response is not necessary to support a healthy pregnancy.

- Oppenheim, S. M., Moyer, A. L., Bondurant, R. H., Rowe, J. D. & Anderson, G. B. *Theriogenology* **54**, 629–639 (2000).

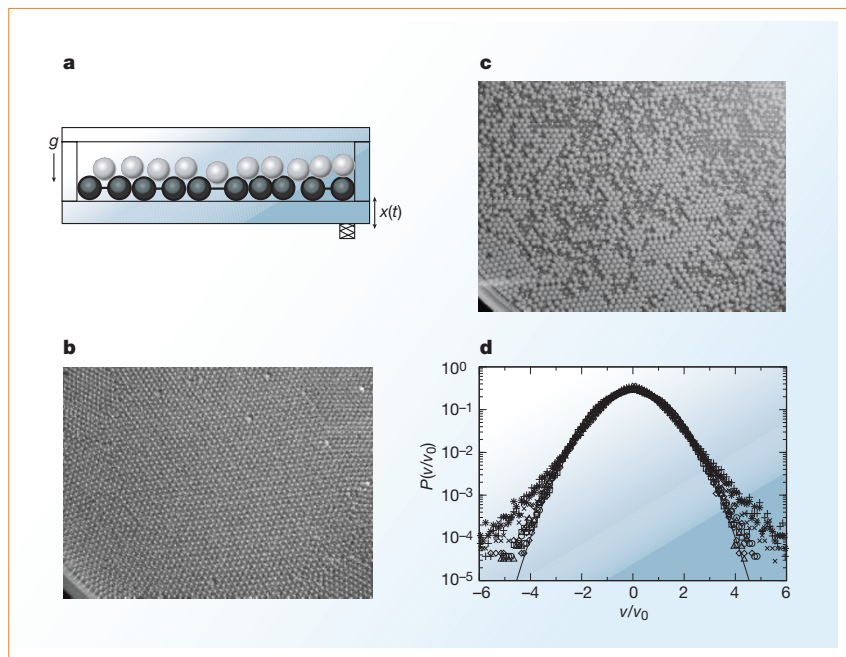


Figure 1 The two-layered granular system. **a**, Geometry of the experimental set-up; the accelerometer is shown at the bottom, on the right. **b**, Photograph of the dimeric layer: diameter of spheres, 3.2 mm; dimer mass, 185 mg. Note the extensive ordered region. **c**, Photograph of white Delrin balls (coverage (c) = 0.4) at rest on top of the dimer layer (roughly one-sixth of the cell is shown). **d**, Velocity statistics for the first- and second-layer grains, for dimensionless acceleration $\Gamma = 2.0$. The distribution of the first-layer grains is non-gaussian. First layer: crosses, $f = 70$ Hz, $c = 0.40$; plus symbols, $f = 50$ Hz, $c = 0.60$; asterisks, $f = 90$ Hz, $c = 0.60$. For the second-layer grains, the renormalized distribution is independent of system parameters within the range studied and is nearly gaussian (solid line) in shape. Second layer: diamonds, $f = 70$ Hz, $c = 0.40$; squares, $f = 50$ Hz, $c = 0.60$; circles, $f = 90$ Hz, $c = 0.60$; triangles, $f = 70$ Hz, $c = 0.80$.